Theoretical and Applied Fracture Mechanics 116 (2021) 103119

Contents lists available at ScienceDirect

Theoretical and Applied Fracture Mechanics

journal homepage: www.elsevier.com/locate/tafmec

An assessment of different approaches for measuring crack sizes in fatigue and fracture mechanics specimens☆

E. Lucon

Applied Chemicals and Materials Division, National Institute of Standards and Technology (NIST), Boulder, CO, United States

ARTICLE INFO

Keywords:
Area Average Method
Fatigue tests
Final crack size
Fracture toughness tests
Initial crack size
Master Curve

ABSTRACT

Several fatigue and fracture mechanics test standards prescribe the use of fatigue precracked specimens, and measured initial and final crack sizes are required for the analyses. All these test methods utilize the X-Point Average Method, with X = 2 ÷ 9, for measuring crack sizes, but another approach, the Area Average Method, is also often used for the same purpose. This investigation compared the two measurement approaches on 140 fracture toughness tests performed on various materials and specimen types, both in the ductile-to-brittle transition (Master Curve) and upper shelf (*J-R* tests) fracture regimes. Results obtained fully support the inclusion of the Area Average Method in all test standards requiring crack size measurements.

1. Introduction

Many mechanical tests [1] require actual physical defects (cracks) in test specimens, rather than sharp machined notches. Specifically, fracture mechanics specimens must contain actual cracks, typically produced by fatigue cycling (precracking) before the actual fracture toughness test. Fatigue precracking must be performed with the material in the final heat treat condition, and in the case of neutron-exposed materials preferably in the irradiated condition, and before any side-grooving is conducted. Other examples that require precracked specimens are tests for the measurement of fatigue crack growth rates (da/dN vs. ΔK) [2] and creep crack growth tests [3].

The size (length) of the crack initially present in the test specimen (initial crack size, a_0) is then used in the calculation of test results, along with the final crack size (a_f) for those tests where stable crack extension/growth occurs. Test standards contain provisions for the measurement of crack sizes in accordance with a specific methodology, as well as validity requirements for the shape/configuration of the measured crack front/contour.

The most commonly used approach is, by far, the *X*-Point Average Method, where *X* indicates the number of local crack size measurements that are averaged to derive the values of a_0 and a_f to be used in the analyses. The values of *X* prescribed by various ASTM Test Methods are:

- $X = 2$ for fatigue crack growth specimens (surface crack measurements); E647 [2] also allows $X = 3$, with an additional measurement taken at mid-thickness of the specimen.
- $X = 3$ for K_{Ic} (plane-strain fracture toughness) measurements [4], K_R curve determination [5], K_{Ia} crack arrest toughness tests [6], and crack resistance tests under low-constraint conditions for specimens thinner than 5 mm [7]. Environment-assisted fatigue cracking tests [8] also prescribe $X = 3$. Crack size measurements are generally taken at mid-thickness, ¼ thickness, and ¾ thickness, where the thickness for side-grooved specimens corresponds to the distance between side-groove roots (net thickness). Note that this approach is also adopted by ISO 12737:2005 for the determination of plane-strain fracture toughness [9].
- $X = 5$ for creep-fatigue crack growth tests [10] and crack resistance tests under low-constraint conditions for specimens thicker than 5 mm [7]. Measurements are taken at equally spaced positions along the specimen thickness or net thickness.
- $X = 9$ is required by fracture toughness tests in the ductile-to-brittle transition region [11] and under fully ductile conditions [12], as well as for creep crack growth tests [3]. Note that "9-Point Average" is not specifically mentioned in either E1820 or E1921, but this is how the method is commonly referred to inside the fracture testing community.

As can be noted, the number of crack size measurements varies greatly between different test methods, which ostensibly require

☆ This work is an official contribution of the National Institute of Standards and Technology and is not subject to copyright in the United States.

E-mail address: enrico.lucon@nist.gov.

https://doi.org/10.1016/j.tafmec.2021.103119
Received 18 August 2021; Received in revised form 12 September 2021; Accepted 29 September 2021
Available online 4 October 2021
0167-8442/Published by Elsevier Ltd.

different accuracy in tracing the actual contour of crack fronts for their calculations. This paper will focus on the 9-Point Average (9PA) Method prescribed by E1820 [12] and E1921 [11].

1.1. 9-point average (9PA) method

This method uses 9 equally spaced measurement locations across the specimen thickness or net thickness, centered about the specimen centerline and extending to 0.005 W (W = specimen width) from the root of the side-grooves or the surfaces of plane-sided specimens (accounting for any lateral contraction). Initial and final crack sizes are determined by a weighted average, where the two near-surface measurements (a_1 and a_9) are given a lower weight than the remaining seven measurements:

$$a = \frac{\left(\frac{a_1+a_9}{2}\right) + \sum_{i=2}^{8} a_i}{8} \quad (1)$$

An example of the 9-Point Average Method applied to the measurement of initial and final crack sizes on a plane-grooved Compact Tension, 1TC(T), specimen is illustrated in Fig. 1 (left side).

From a practical point of view, the operator measures the minimum specimen thickness (for plane-sided specimens) or net thickness (for side-grooved specimens), then subtracts from it $2 \times 0.005\ W = 0.01\ W$, and finally divides the value obtained by X-1 (8 in the case of E1820/E1921).

For example, assuming a 1TC(T) specimen with nominal width W = 50 mm and minimum thickness B_{min} = 25 mm, one has 25 – 0.01 × 50 = 24.5 mm, and 24.5/8 = 3.0625 mm. The 9 measurement positions across the net thickness are given by (with the lateral surface corresponding to $x = 0$): $x_i = (i - 1) \times 3.0625$ mm, with $i = 1, \ldots, 9$.

In E1820 and E1921, each of the 9 crack size measurements must fulfil the following validity requirement: the maximum difference between an individual measurement, a_i, and the calculated average cannot exceed $0.1\sqrt{b_0 B_N}$, where b_0 is the initial ligament size ($b_0 = W\text{-}a_0$).

1.2. Area Average (AA) Method

An alternative approach for measuring crack sizes, used in several published studies, is the Area Average (AA) Method, which consists in measuring the surface area of a region delimited by a reference line[1] and the initial or final crack front. Simply put, the area to be measured corresponds to a specific fracture appearance, corresponding to the type of crack propagation – fatigue, brittle fracture, or ductile fracture – and any possible coloring caused by exposure to high temperatures. By dividing this area by the specimen thickness or net thickness, an estimate of the crack size is obtained, averaged on the whole crack front rather than on a finite number of measurement locations.

The AA Method is illustrated in Fig. 1 (right side). As an example, if the minimum thickness is B_{min} = 24.92 mm and the yellow and black areas in the figures correspond to 627 mm^2 and 88 mm^2 respectively, the initial crack size will be 627/24.92 = 25.16 mm and the final crack size will be (627 + 88)/24.92 = 28.69 mm.

This method is currently not implemented in any ASTM or ISO mechanical test method.

The objective of this investigation is to compare the two measurement methods (9PA and AA) in terms of fracture mechanics test results, and to ultimately assess whether the AA method should also be included in ASTM and ISO test standards as an option for measuring crack sizes in precracked fracture and fatigue test specimens.

[1] As mentioned in the caption of Fig. 1, the reference line corresponds to the zero line for crack size measurements for a specific specimen type (e.g., centerline of pin holes for C(T) specimens; front face for bend, SE(B), specimens).

2. Overview of the investigation

This investigation focused on fracture toughness data obtained in the ductile-to-brittle transition (analyzed in accordance with ASTM E1921) and in the fully ductile, or upper shelf, regime (analyzed in accordance with ASTM E1820).

Transition data are K_{Jc} toughness values corresponding to unstable fracture (cleavage), which are statistically analyzed with the Master Curve method [13] in order to derive the reference temperature, T_0, corresponding to a median toughness of 100 MPa$\sqrt{m}$ for a 1TC(T) specimen. The influence of the crack size measuring method was evaluated on both individual K_{Jc} values and calculated T_0.

Nine data sets were evaluated, corresponding to a total of 91 K_{Jc} tests and the following 5 different specimen types:

- C(T) specimens with ½" (25 mm) thickness, or 0.5TC(T);
- miniaturized C(T) specimens with 4 mm thickness, or MC(T);
- precracked Charpy-type specimens, or PCCv;
- single-edge bend specimens with 20 mm thickness and 40 mm width, or SE(B) 20 × 40;
- miniature bend bars with 1.65 mm thickness and 3.3 mm width, or MSE(B).

Materials considered ranged from a reactor pressure vessel (RPV) base and weld material to reduced-activation ferritic-martensitic (RAFM) steels[2] used for fusion applications.

In the upper shelf regime, 49 tests were evaluated. Specimen geometries and sizes included:

- 1TC(T) specimens (thickness = 25 mm);
- PCCv specimens, both plane-sided and 20% side-grooved;
- SE(B) 20 × 40 specimens;
- SE(B) specimens with 12.5 mm thickness and 25 mm width, or SE(B) 12.5 × 25;
- plane-sided miniaturized precracked Charpy specimens of the KLST type (thickness = 3 mm, width = 4 mm), or PKLST.

Tests had been performed in accordance with ASTM E1820 for the obtainment of the plane-strain fracture toughness (J_Q) and the crack resistance curve (J-R curve). Both multiple-specimen data sets (E1820 basic procedure) and single-specimen analyses (elastic compliance, electric potential drop, and normalization data reduction) were considered.

Materials include A533B RPV steel, additively manufactured (AM) Ti6Al4V, T-200 maraging steel, and pipeline steels (API X65 and X100, base and weld metals).

Crack size measurements (only a_0 for transition tests; both a_0 and a_f for upper shelf tests) were obtained from digital pictures of the fracture surfaces by means of *ImageJ*, a freely available Java-based image processing program[3] developed at the National Institutes of Health and the Laboratory for Optical and Computational Instrumentation [14,15]. Using *ImageJ*, the implementation of both 9PA and AA methods was relatively straightforward.

The quality of the digital pictures varied greatly, reflecting real situations where low-resolution photos might have to be analyzed, adding up to the overall uncertainty of the measurements.

[2] RAFM steel data were kindly provided by X. Chen from Oak Ridge National Laboratory (ORNL).

[3] Certain commercial equipment, instruments, software packages, or materials are identified in this document in order to specify the experimental procedure adequately. Such identification is not intended to imply recommendation or endorsement by the National Institute of Standards and Technology, nor is it intended to imply that the materials or equipment identified are necessarily the best available for the purpose.

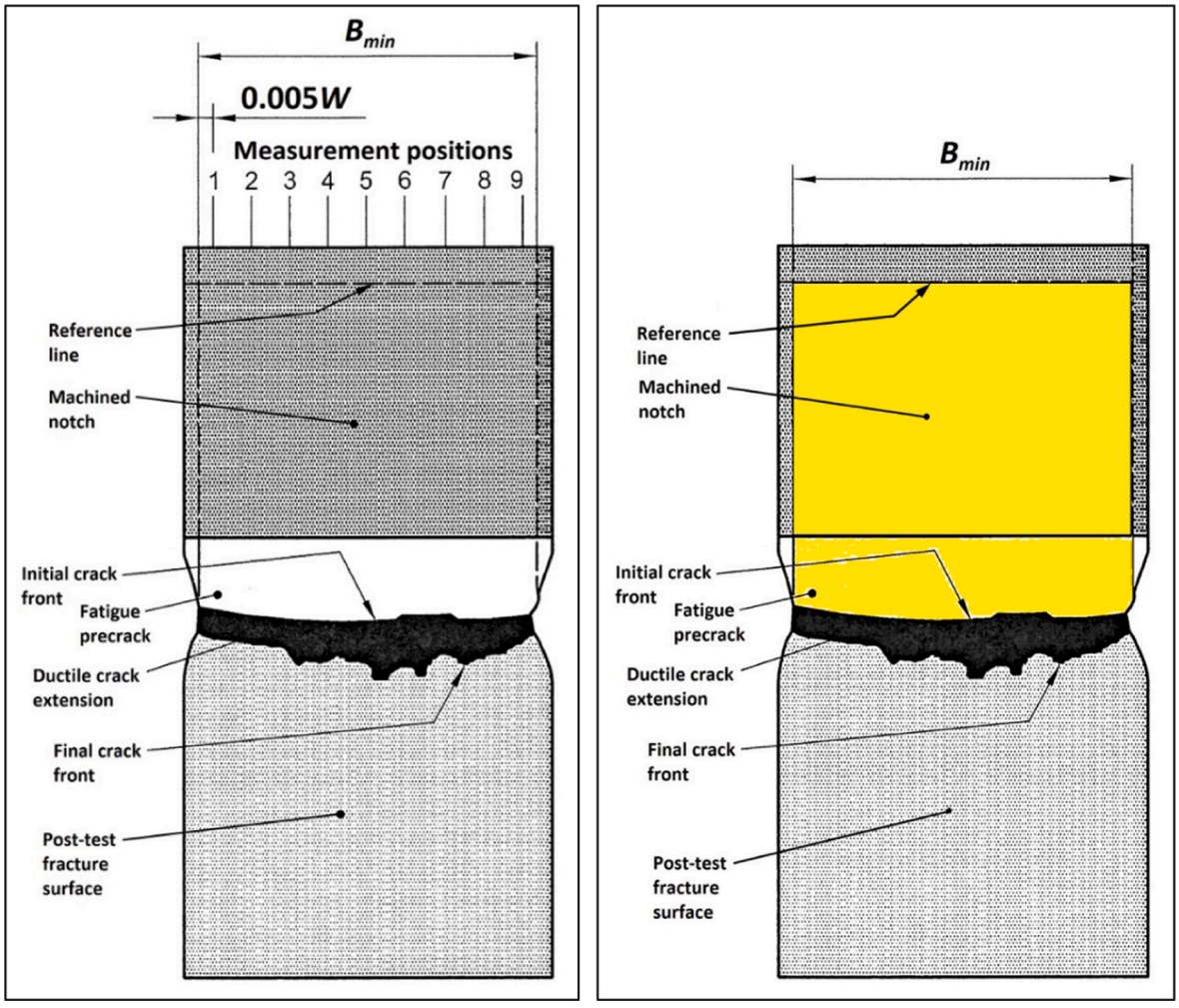

Fig. 1. Illustration of the 9-Point Average Method (left) and Area Average Method (right) for measuring a_0 and a_f on a plane-sided C(T) specimen. The reference line corresponds to the centerline of the pin holes. For the AA Method, a_0 is obtained by dividing the yellow area by B_{min}, while a_f is obtained by dividing the sum of the yellow and black areas by B_{min}. (For interpretation of the references to colour in this figure legend, the reader is referred to the web version of this article.)

Finally, three distinct situations were encountered:

(a) specimens where either 9pA or AA crack size measurements had already been performed by the author at the time tests were performed;
(b) specimens where no measurements were available, and both methods had to be applied in the framework of this study; and
(c) specimens for which 9pA measurements had already been performed by the original data owner (X. Chen of ORNL), and only AA measurements had to be obtained by the author.

It is reasonable to assume that situation (b), whereby measurements were performed by the same individual (author) in the same time frame, could be associated to the highest precision. Conversely, situation (c) (different individuals using different methods) should result in the lowest precision.

3. Results obtained

3.1. K_{Jc} tests in the transition regime (Master Curve analyses)

Nine data sets, comprising 91 fracture toughness tests, were analyzed to establish the influence of the crack size measuring method on individual K_{Jc} results and Master Curve reference temperature, T_0.

A summary of the results obtained is provided in Table 1, while detailed results are given in Appendix A.

Table 1
Results obtained for K_{Jc} tests.

Material	Specimen type	N	$\Delta a_{0,MAX}$		$\Delta K_{Jc,MAX}$	ΔT_0
			(mm)	(%)	(%)	(°C)
RAFM-1	MC(T)	10	0.171	4.29	5.43	−0.30
	0.5TC(T)	7	0.215	1.80	1.17	−0.49
	MSE(B)	16	0.033	2.01	2.08	0.09
RAFM-2	MC(T)	11	−0.221	−5.79	−3.47	0.02
	0.5TC(T)	6	0.181	1.44	1.38	−0.17
	MSE(B)	16	0.057	3.36	3.86	−0.48
A508 base	PCCv	10	0.142	2.63	3.22	0.00
A508 weld		5	0.035	0.67	0.33	0.01
	SE(B) 20 × 40	10	0.268	1.27	−2.05	−0.08

N = number of tests in the data set.
$\Delta a_{0,MAX}$ = largest difference between $a_{0,9PA}$ and $a_{0,AA}$ (absolute and relative) [Here and in the rest of the paper, absolute differences are calculated by subtracting the AA value from the 9PA value; relative differences are obtained by dividing absolute differences by the 9PA value (assumed to be the "reference").].
$\Delta K_{Jc,MAX}$ = largest difference between $K_{Jc,9PA}$ and $K_{Jc,AA}$ (relative).
ΔT_0 = difference between $T_{0,9PA}$ and $T_{0,AA}$ (absolute).

Across the 91 tests examined, a_0 differences between 9PA and AA methods ranged between –0.252 mm and 0.268 mm, with an average of

0.028 mm. The largest relative deviation was −5.79% and the average relative deviation was 0.5%.

In terms of fracture toughness at unstable fracture, K_{Jc}, the largest relative difference was 5.4% and the average relative deviation was 0.5%.

As far as Master Curve reference temperatures, T_0, are concerned, differences ranged between −0.49 °C and 0.09 °C and the average difference corresponded to −0.156 °C.

Values of K_{Jc} yielded by 9PA and AA measurements are compared in Fig. 2, differentiated by specimen type and assessed with respect to ±5% agreement limits.

3.2. Fracture toughness tests in the upper shelf regime

Elastic-plastic fracture toughness tests per ASTM E1820 can be conducted and analyzed according to one of the following procedures:

- Basic procedure: several nominally identical specimens are tested to different values of applied force and load-line or crack mouth opening displacement, so that every test provides a single J-Δa data point on the crack resistance curve, from which a value of critical toughness (J_Q or J_{Ic})[4] is calculated. This approach is known as multiple-specimen technique.
- Resistance curve procedure: each individual specimen provides a single crack resistance curve and corresponding critical toughness. For this, a technique for monitoring stable crack propagation during the test is required. The following crack monitoring techniques can be applied: elastic compliance (EC), direct current electric potential difference (DCEPD), and normalization data reduction (NDR). These methods are collectively denominated single-specimen techniques.

3.2.1. Multiple-specimen tests

Five multiple-specimen data sets were considered in our investigation, comprised of 34 tests on PKLST and PCCv specimens of T200 maraging steel and API X65 pipeline steel. For each of the tests, the influence of the crack size measuring method was investigated on the initial crack size, a_0, the final crack size, a_f, the resulting crack extension $\Delta a = a_f - a_0$, and the value of J-integral at test end, J_i. For the whole data set, the critical toughness, J_Q, corresponding to 9PA and AA was calculated.

Table 2 presents a summary of the results obtained. Individual test results are reported in Appendix B.

Initial crack profiles (which are generated by fatigue precracking) are generally much smoother and more regular than final crack profiles, which for some materials can be significantly jagged and uneven (see Fig. 1 for an example). Hence, larger uncertainties and differences between 9PA and AA a_f measurements can be expected: this is confirmed by Table 2. Calculated crack extensions, Δa, predictably exhibited the largest deviations as a result of the summation of differences/uncertainties in both a_0 and a_f values.

In terms of J_i, crack size measurements using the AA method tend to yield slightly lower values (average difference among the 5 data sets: −1.0%). As far as the provisional critical fracture toughness, J_Q, is concerned, this slightly conservative trend is retained, with an average difference of –2.8%. Deviations for the individual data sets range between −9.3% and 11.1%.

3.3. Single-specimen technique: Elastic Compliance (EC) tests

Fifteen EC tests on 1TC(T), PCCv, and SE(B) 12.5 × 25 specimens were analyzed (summary in Table 3, individual results in Appendix B).

For tests conducted using the Elastic Compliance technique for monitoring crack extension in accordance with ASTM E1820, only the first value of J-integral uses the measured initial crack size. All remaining J values are calculated from crack sizes obtained from measured elastic compliances during unload/reload cycles. Δa values are obtained as the difference between the compliance-derived crack size and the initial predicted crack size, a_{0q}, which is obtained by fitting J_i and a_i data points before maximum force. The measured final crack size is not used in calculations at all.

It is therefore evident that in EC toughness tests optical crack size measurements play a very marginal role in calculations, and are mostly used for the following validity requirements:

(a) The optically measured initial crack size must not differ from a_{0q} by more than the larger of 0.01 W or 0.5 mm.
(b) The difference between predicted and measured crack extension must not exceed 15% of the measured Δa (for $\Delta a < 0.2\ b_0$) or 3% b_0 (for $\Delta a \geq 0.2\ b_0$).

It's therefore to be expected that no significant influence of crack size measurement method is observed on critical toughness EC tests, as confirmed by Table 3.

In terms of the validity requirements listed above, only for 3 of the 15 tests analyzed (20%) the fulfilment or non-fulfilment of requirements (a) and (b) above changes when AA measurements are used instead of 9PA. Specifically, for one of the 1TC(T) tests on A508 base the difference between a_o and a_{oq} is unacceptable for 9PA and acceptable for AA; and for two of the SE(B) 12.5 × 25 tests on X100 weld, the difference between predicted and measured crack extension is unacceptable for 9PA and acceptable for AA. Hence, a slightly favorable effect of the AA method on test validity was observed for EC tests.

3.3.1. Single-specimen technique: Direct current electric potential difference (DCEPD) tests

Four of the specimens investigated (all 20% side-grooved PCCv) had also been instrumented to monitor crack extension in terms of electrical potential variation across the crack plane (DCEPD technique). The effect of crack size measurement method on each specimen is shown in Table 4. Additional details are provided in Appendix B.

DCEPD tests were analyzed according to the provisions contained in Annex A18 of E1820. All the relationships between potential difference and crack size reported in the annex contain the blunting-corrected initial crack size, $a_{0,bl}$, which is obtained by adding a correction to the measured a_0 in order to account for crack-tip blunting before the onset of ductile crack extension. Moreover, predicted crack sizes must be adjusted based on the measured initial crack size and the measured crack extension, $a_f - a_0$, in order to improve the overall accuracy of the predictions. It is therefore evident that the crack size measurement method for a DCEPD can have a much more significant influence than for an EC test, as shown by the last column in Table 4. It is also interesting to note that in all cases, $J_{Q,AA}$ values are lower (more conservative) than $J_{Q,9PA}$.

3.3.2. Single-specimen technique: Normalization data reduction (NDR) tests

This study analyzed 14 of the 49 fully ductile fracture tests considered in this study, all on 20% side-grooved PCCv specimens, using the NDR technique, which is described in Annex A15 of E1820. Using this methodology, a J-R curve is obtained directly from a force/displacement record, together with initial and final crack size measurements. Specifically, each value of force and load-line or crack mouth opening displacement, except the final force/displacement pair, is normalized using a blunting-corrected crack size that contains a_0. The final force/displacement pair is normalized using the measured final crack size, a_f. The principle of this procedure is similar to the crack size adjustment

[4] If the critical toughness is found to be independent of the specimen size, the critical value of the J-integral is denominated J_{Ic}. Otherwise, it is labeled J_Q (provisional and size-dependent fracture toughness).

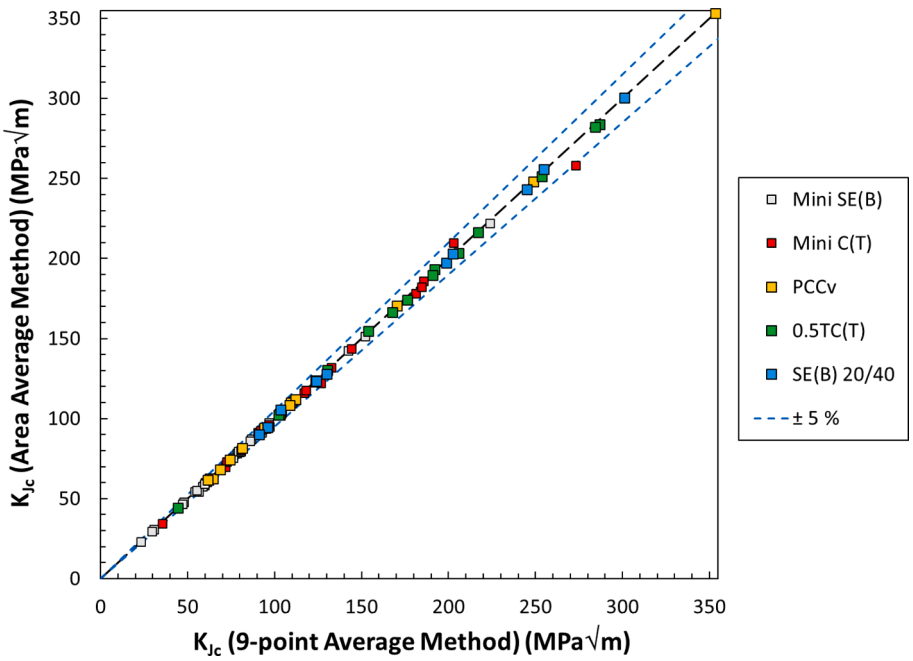

Fig. 2. Comparison between fracture toughness at cleavage, K_{Jc}, obtained from 9PA and AA measurements of initial crack size for the 91 tests in the ductile-to-brittle transition region.

Table 2
Results obtained for the *J-R* data sets (multiple-specimen approach).

Material	Specimen type	*N*	$\Delta a_{0,MAX}$		$\Delta a_{f,MAX}$		$\Delta[\Delta a]_{MAX}$		$\Delta J_{i,MAX}$	ΔJ_Q
			(mm)	(%)	(mm)	(%)	(mm)	(%)	(%)	(%)
T200	PKLST	5	−0.046	−2.46	0.190	6.40	0.161	17.29	−3.69	−9.3
	PCCv 20 %SG	5	−0.038	−0.77	−0.132	−2.35	−0.073	−15.74	0.80	11.1
	PCCv PS	4	−0.112	−2.13	−0.084	−1.32	0.110	10.27	−4.63	−4.6
X65	PKLST	5	0.035	1.86	0.087	2.83	0.090	9.94	−1.33	−4.2
	PCCv 20 %SG	15	−0.107	−2.19	0.272	3.65	0.285	–32.97	−3.26	−7.0

$\Delta a_{f,MAX}$ = largest recorded difference between $a_{f,9PA}$ and $a_{f,AA}$ (absolute and relative).
$\Delta[\Delta a]_{MAX}$ = largest calculated difference between Δa_{9PA} and Δa_{AA} (absolute and relative).
$\Delta J_{i,MAX}$ = largest recorded difference between $J_{i,9PA}$ and $J_{i,AA}$ (relative).
ΔJ_Q = difference between $J_{Q,9PA}$ and $J_{Q,AA}$ (relative).
20 %SG = 20% side-grooved.
PS = plane-sided.

Table 3
Results obtained for the single-specimen tests conducted with the Elastic Compliance technique.

Material	Specimen type	*N*	$\Delta a_{0,MAX}$		$\Delta a_{f,MAX}$		$\Delta[\Delta a]_{MAX}$		$\Delta J_{Q,MAX}$
			(mm)	(%)	(mm)	(%)	(mm)	(%)	(%)
A508 base	1TC(T)	3	0.267	1.05	0.742	2.55	0.639	16.17	0.00
AM Ti6Al4V	PCCv 20% SG	6	−0.050	−0.99	−0.088	−1.48	−0.058	5.02	0.01
X100 weld	SE(B) 12.5 × 25	6	0.186	1.44	0.706	4.56	0.591	22.23	0.00

$\Delta J_{Q,MAX}$ = largest difference between $J_{Q,9PA}$ and $J_{Q,AA}$ (relative).

Table 4
Results obtained for the single-specimen tests conducted with the DCEPD technique.

Material	Specimen type	$J_{Q,9PA}$ (kN/m)	$J_{Q,AA}$ (kN/m)	ΔJ_Q (%)
T200 maraging steel	PCCv 20% SG	601.14	515.04	14.3
		687.31	622.09	9.5
		692.07	565.51	18.3
X65		390.35	384.42	1.5

prescribed by ASTM E1820, Annex A18, for DCEPD tests.

Therefore, the influence of the crack size measurement method can be expected to be as significant as for DCEPD results, as confirmed by Table 5. Individual analyses are also provided in Appendix B. In this case, however, no real trend toward conservatism or non-conservatism is visible; J_Q differences between 9PA and AA range between −24.5% and 24.0%, with a mean difference of −0.4%.

3.4. Crack profile validity

According to both E1820 and E1921, individual measurements of

Table 5
Results obtained for the single-specimen tests analyzed with the NDR technique.

Material	Specimen type	$J_{Q,9PA}$ (kN/m)	$J_{Q,AA}$ (kN/m)	ΔJ_Q (%)
AM Ti6Al4V	PCCv 20% SG	122.99	124.02	−0.8
		104.45	103.51	0.9
		120.54	120.41	0.1
		164.74	182.69	−10.9
		197.78	197.81	0.0
T200 maraging steel		354.95	335.83	5.4
		610.80	616.25	−0.9
X65		783.25	811.27	−3.6
		1681.86	1763.50	−4.9
		1182.77	1472.49	−24.5
		1649.92	1272.34	22.9
		1346.86	1023.61	24.0
		1718.42	1848.50	−7.6
		1239.76	1313.22	−5.9

initial and final crack size cannot differ from their respective average values by more than $0.1\sqrt{b_0 B_N}$.

This requirement was checked against all crack size measurements for the 140 specimens considered in the study, both for the 9-Point Average Method and the Average Area Method.

For 9PA, the requirement was applied to the minimum and maximum among a_i values. For AA, the minimum and maximum distances between the specimen reference line and the initial or final crack front were considered. Moreover, to ensure better consistency with 9PA, minimum and maximum distances were determined after excluding the first 0.005 W from the root of each side-groove or side surface of plane-sided specimens. For the example of Fig. 1, the measurements that were checked against the standard requirement are shown in Fig. 3.

The results of the crack profile validity checks are summarized in Table 6, and show that the AA method is generally more restrictive than the 9PA method. This was expected, as the "discrete" nature of the latter approach can cause the measurement locations to miss specific features (peaks/valleys) of the crack front, which are instead always captured by the "continuous" nature of AA. This is particularly true in case of final cracks (92% valid for 9PA, only 49% for AA), which are often more jagged and irregular than initial cracks (84% valid for 9PA, 69% for AA).

4. Discussion

Initial crack sizes measured on all 140 specimens using the two methods are compared in Fig. 4, while the same comparison is provided in Fig. 5 for final crack sizes for the 41 ductile specimens.

Of the 140 specimens analyzed in this study, only one (0.7% of the analyzed specimens) exhibited a difference between a_0 measured with 9pA and AA greater than 5%. In no case the difference exceeded 0.25 mm for specimens with less than ½" (12.5 mm) thickness (MSE(B), MC (T), PKLST, and PCCv), or 0.5 mm for specimen thicker than ½" (12.5 mm) (SE(B) 12.5 × 25, 0.5TC(T), SE(B) 20 × 40, 1TC(T)).

As far as a_f is concerned, out of 49 fully ductile fracture tests, 4 specimens (8.2%) yielded differences greater than 0.25 mm or 0.5 mm depending on thickness, and only for one specimen (2%) the difference exceeded 5%.

Turning our attention to the results of the fracture toughness tests, it was already shown in Fig. 2 that only for one (1.1%) of the 91 Master Curve tests the crack size measurement method caused a different in K_{Jc} larger than 5%. In terms of reference temperature, T_0, the influence of the crack size measurement method is insignificant (less than 0.5 °C, see Table 1).

For the 29 upper shelf tests conducted with the multiple-specimen approach, J_i differences lower than 5% were calculated (Fig. 6).

Finally, values of critical toughness, J_Q, were calculated for crack sizes measured with the two different approaches in accordance with both multiple-specimen (4 data sets) and single-specimen (EC – 13 tests; DCEPD – 4 tests; NDR – 14 tests) approaches. As illustrated in Fig. 7, for 91.4% of the tests (32 out of 35 tests) critical values J_Q differ by less than ±20%, which is the typical scatter band for J-based critical toughness measured per ASTM E1820 [16]. Deviations between 9PA and AA-based results tend to increase with toughness level. The three tests exhibiting differences outside ±20% are all NDR tests, which rely heavily on both initial and final measured crack sizes for the normalization of force and displacement values.

Aside from the comparisons between crack sizes or toughness test results, it is the author's opinion that there is no technical reason to consider the Area Average Method inferior to, or less reliable than, the X-Point Average Method (X = number of measurement positions). For highly irregular crack fronts (which might however be invalid anyway),

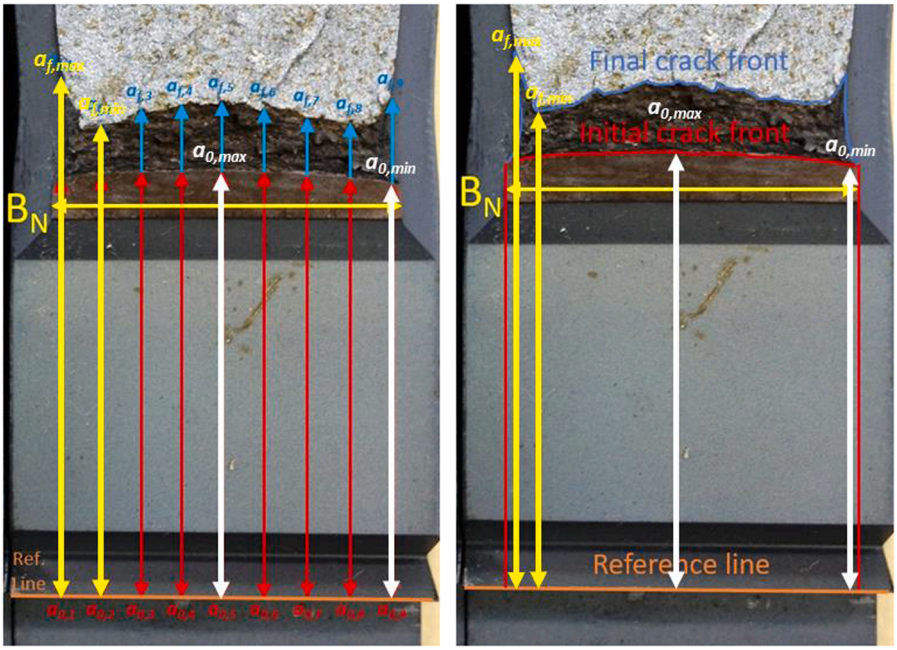

Fig. 3. Identification of the minimum and maximum crack sizes for the 9-Point Average Method (left) and the Area Average Method (right).

Table 6
Crack profile validity for 9PA and AA measurements.

Test type	Material	Specimen type	*N*	9PA		AA		*N*	9PA		AA	
				Initial crack size					Final crack size			
				Valid	Invalid	Valid	Invalid		Valid	Invalid	Valid	Invalid
K_{Jc}	FM-1	MC(T)	10	1	9	1	9	–	–	–	–	–
		0.5TC(T)	7	6	1	5	2	–	–	–	–	–
		MSE(B)	16	16	0	16	0	–	–	–	–	–
	FM-2	MC(T)	11	4	7	5	6	–	–	–	–	–
		0.5TC(T)	6	4	2	4	2	–	–	–	–	–
		MSE(B)	16	15	1	15	1	–	–	–	–	–
	A508 base	PCCv 20 %SG	10	10	0	10	0	–	–	–	–	–
	A508 weld		5	5	0	5	0	–	–	–	–	–
		SE(B) 20 × 40	10	10	0	10	0	–	–	–	–	–
J_Q/*J-R*	A508 base	1TC(T)	3	3	0	3	0	3	3	0	2	1
	AM Ti6Al4V	PCCv 20 %SG	6	6	0	6	0	6	6	0	5	1
	X100 weld	SE(B) 12.5 × 25	6	6	0	1	5	6	5	1	1	5
	T-200	PCCv 20 %SG	5	4	1	0	5	5	5	0	0	5
		PCCv PS	4	3	1	1	3	4	3	1	0	4
		PKLST	5	5	0	1	4	5	3	2	1	4
	X65	PCCv 20 %SG	15	15	0	13	2	15	15	0	14	1
		PKLST	5	5	0	1	4	5	5	0	1	4
		TOTAL	**140**	**118**	**22**	**97**	**43**	**49**	**45**	**4**	**24**	**25**
				84%	**16%**	**69%**	**31%**		**92%**	**8%**	**49%**	**51%**

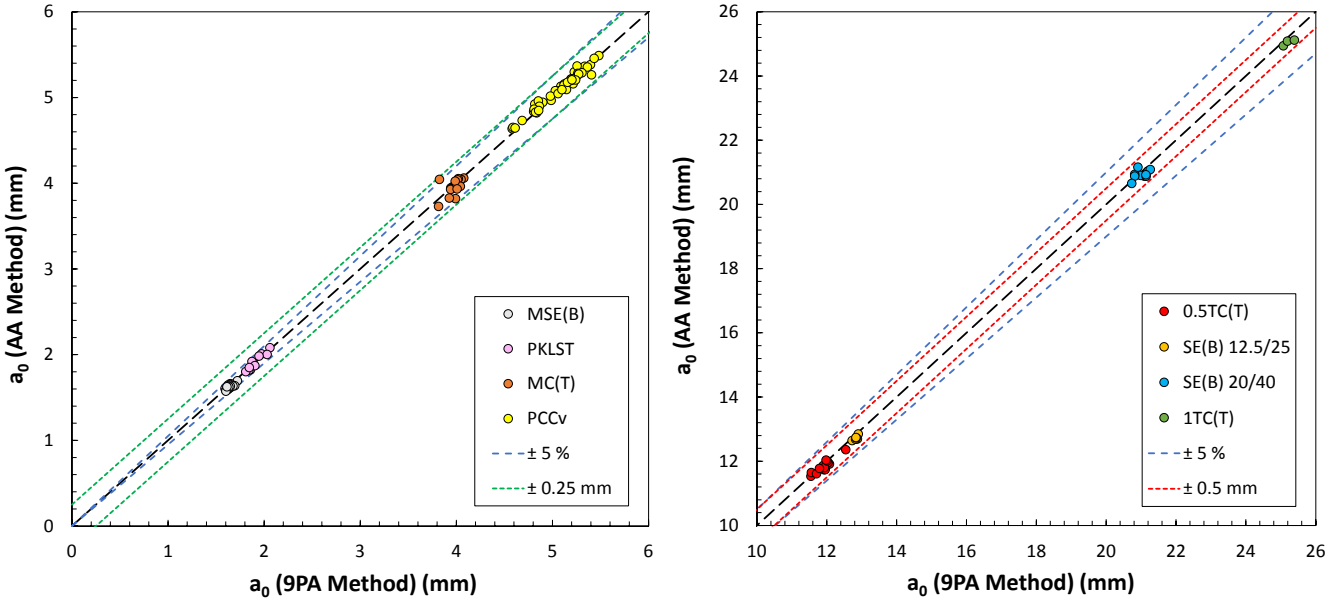

Fig. 4. Comparison between 9PA and AA initial crack sizes (140 specimens). Left side: specimens with thickness lower than 1/2″ (12.5 mm); Right side: specimens with thickness between ½" and 1″ (25 mm).

AA could provide a better characterization of the actual crack profile than *X*PA, which might "miss" specific features such as peaks and valleys, unless they happen to correspond to one of the measurement locations. And this tends to be exacerbated for low values of X , namely $X \leq 5$. This is also the reason why AA tends to be stricter than *X*PA in identifying invalid crack fronts, as detailed in Section 3.3 above.

The author therefore recommends the inclusion of the Area Average Method in all fracture and fatigue test standards that require accurate measurements of initial and final crack size, as an alternative to the well-established *X*-Point Average Method.

An additional benefit of adopting the AA methodology would be facilitating better consistency among the various test standards, which currently prescribe averaging measurements taken at a number of locations ranging between 2 and 9 along the crack front.

5. Conclusions

This investigation compared two methodologies for measuring initial and final crack sizes in mechanical test specimens, namely the *X*-Point Average Method (with X = number of measurement positions, ranging between 2 and 9 depending on the test method) and the Average Area Method. Presently, only the former method is standardized.

Comparisons were conducted on 91 fracture toughness tests in the ductile-to-brittle transition region (analyzed in accordance with ASTM E1921 – Master Curve approach) and 49 tests in the fully ductile regime (analyzed in accordance with ASTM E1820, using various multiple- and single-specimen techniques).

The results obtained show close agreement between measured crack sizes, particularly for initial cracks obtained by fatigue precracking. The influence of the measurement method on fracture test results depends

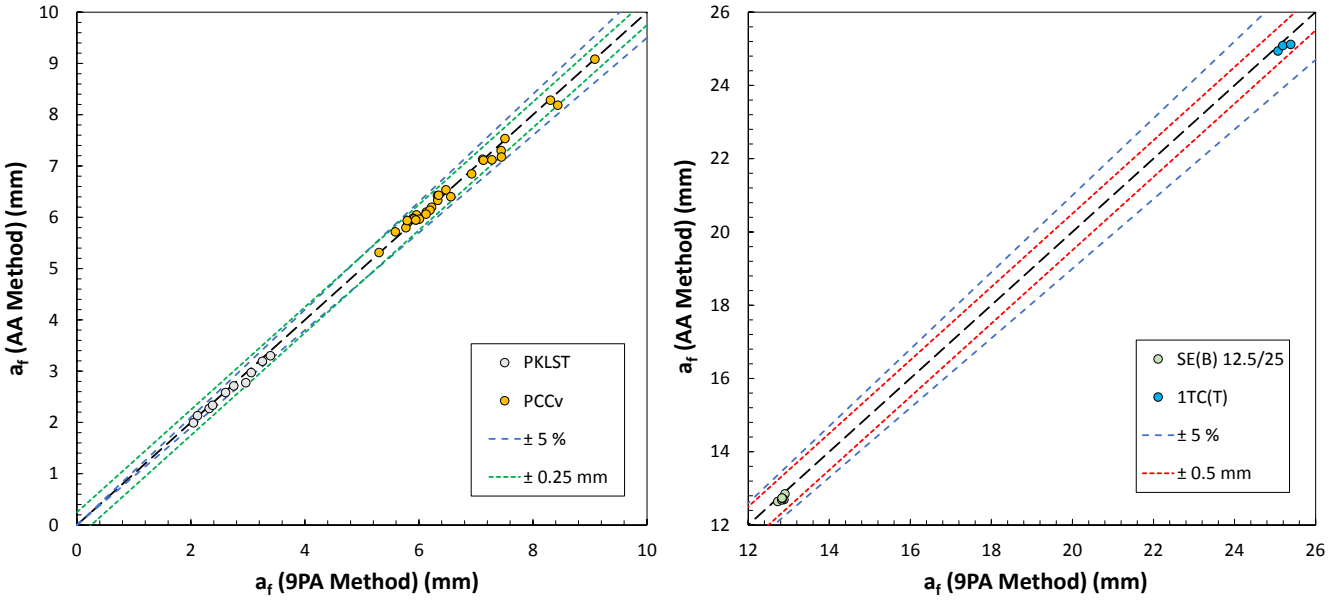

Fig. 5. Comparison between 9PA and AA final crack sizes (49 specimens). Left side: specimens with thickness lower than 1/2″ (12.5 mm); Right side: specimens with thickness between ½" and 1″ (25 mm).

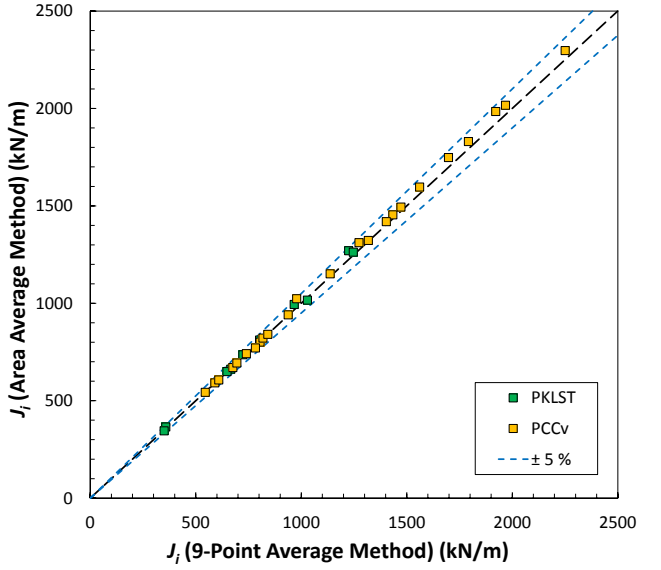

Fig. 6. Influence of crack size measurement method on *J*-integral values, J_i, for the multiple-specimen method.

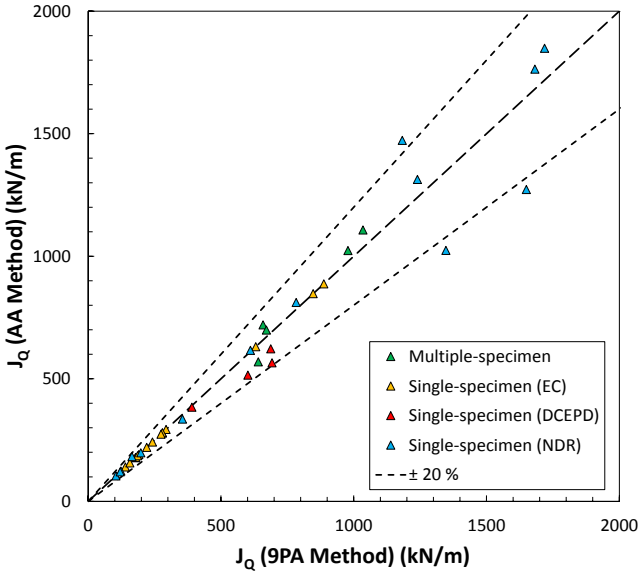

Fig. 7. Influence of crack size measurement method on critical *J*-integral values, J_Q, for elastic–plastic fracture toughness tests.

significantly on how measured crack sizes are used in test analyses. The influence has been found negligible for Master Curve testing and Elastic Compliance *J-R* tests. Other types of upper shelf fracture toughness tests (multiple-specimen, electrical potential difference, and normalization data reduction) are more sensitive to the crack size measurement method used, as crack sizes are more heavily involved in test analyses. In most cases, however, differences are well within the typical scatter band of *J*-integral critical toughness values.

This study therefore supports the inclusion of the Area Average Method in all the ASTM Test Standards that require measuring crack sizes for fatigue and fracture testing, as an alternative to the widely popular *X*-Point Average Method. It is also contended that the Area Average Method can provide a better representation of the actual crack profile, which can be relevant whenever crack front irregularities might affect the validity of the test. However, considering that the AA method is bound to be significantly more restrictive than the *X*PA method, standards committees might also consider whether to relax crack straightness requirements when using AA (or, for that matter, either procedure).

Declaration of Competing Interest

The authors declare that they have no known competing financial interests or personal relationships that could have appeared to influence the work reported in this paper.

Acknowledgments

The author wishes to express his sincere gratitude to Dr. Xiang (Frank) Chen of Oak Ridge National Laboratory for sharing Master Curve

test data and specimen pictures of RAFM steels.

Appendix A. Detailed results for Master Curve tests (91 tests)

Material: **FM steel-1**
Specimen type: **mini-C(T)**

Specimen	Initial crack size, a_0 (mm)				Fracture toughness, K_{JC} (MPa√m)			Reference temperature, T_0 (°C)		
id	9ptA	AA	Δ		9ptA	AA	Δ	9ptA	AA	Δ
EM11	4.031	3.997	0.034	0.85%	273.07	258.23	5.43%			
EM12	3.992	3.821	0.171	4.29%	126.41	122.01	3.48%			
EM13	3.962	3.960	0.002	0.06%	81.79	81.73	0.07%			
EM14	4.078	4.059	0.018	0.45%	116.79	116.30	0.42%			
EM15	4.028	3.994	0.034	0.85%	123.40	122.47	0.76%	-125.8	-125.5	-0.30
EM21	3.961	3.945	0.016	0.40%	132.46	131.78	0.52%			
EM22	4.049	4.045	0.004	0.09%	117.95	117.85	0.09%			
EM23	3.942	3.945	-0.003	-0.07%	185.69	185.77	-0.05%			
EM24	4.021	4.054	-0.033	-0.83%	90.36	91.25	-0.98%			
EM25	4.012	4.040	-0.027	-0.68%	91.75	92.49	-0.80%			

Material: **FM steel-1**
Specimen type: **0.5TC(T)**

Specimen	Initial crack size, a_0 (mm)				Fracture toughness, K_{JC} (MPa√m)			Reference temperature, T_0 (°C)		
id	9ptA	AA	Δ		9ptA	AA	Δ	9ptA	AA	Δ
E56	12.076	11.912	0.164	1.36%	253.55	251.23	0.91%			
E57	11.921	11.736	0.186	1.56%	205.93	203.52	1.17%			
E58	12.040	11.957	0.083	0.69%	167.58	166.57	0.60%			
E59	11.956	11.741	0.215	1.80%	286.94	283.83	1.08%	-171.1	-170.6	-0.49
E5A	11.895	11.864	0.031	0.26%	217.00	216.58	0.19%			
E5B	11.932	11.801	0.131	1.10%	284.14	282.20	0.68%			
E5C	11.547	11.533	0.014	0.12%	130.48	130.33	0.12%			

Material: **FM steel-1**
Specimen type: **mini-bend bars**

Specimen	Initial crack size, a_0 (mm)				Fracture toughness, K_{JC} (MPa√m)			Reference temperature, T_0 (°C)		
id	9ptA	AA	Δ		9ptA	AA	Δ	9ptA	AA	Δ
EB11	1.722	1.696	0.025	1.46%	62.32	61.17	1.85%			
EB12	1.646	1.661	-0.015	-0.91%	30.40	30.91	-1.66%			
EB14	1.593	1.606	-0.013	-0.80%	62.36	62.86	-0.81%			
EB15	1.650	1.617	0.033	2.01%	223.74	221.95	0.80%			
EB21	1.602	1.581	0.021	1.32%	61.23	60.45	1.28%			
EB22	1.611	1.612	-0.002	-0.10%	47.69	47.75	-0.14%			
EB23	1.618	1.618	0.000	-0.02%	110.63	110.64	-0.01%			
EB24	1.605	1.593	0.012	0.76%	108.80	108.32	0.45%	-97.0	-97.1	0.09
EB25	1.622	1.593	0.029	1.78%	59.56	58.32	2.08%			
EB31	1.655	1.659	-0.004	-0.23%	78.36	78.53	-0.21%			
EB32	1.621	1.628	-0.007	-0.43%	29.49	29.70	-0.72%			
EB33	1.648	1.625	0.023	1.39%	80.03	79.09	1.17%			
EB34	1.626	1.630	-0.004	-0.27%	61.21	61.38	-0.28%			
EB35	1.629	1.604	0.026	1.58%	58.59	57.58	1.72%			
EB36	1.647	1.651	-0.004	-0.25%	54.06	54.23	-0.32%			
EB37	1.627	1.645	-0.018	-1.13%	86.63	87.30	-0.78%			

Material: **FM steel-2**
Specimen type: **mini-C(T)**

Specimen	Initial crack size, a_0 (mm)				Fracture toughness, K_{JC} (MPa√m)			Reference temperature, T_0 (°C)		
id	9ptA	AA	Δ		9ptA	AA	Δ	9ptA	AA	Δ
FM11	3.951	3.938	0.013	0.33%	144.14	143.78	0.25%			
FM12	3.953	3.935	0.018	0.46%	104.33	103.88	0.44%			
FM13	4.016	3.956	0.060	1.49%	95.12	93.62	1.58%			
FM14	3.941	3.928	0.013	0.32%	96.58	96.27	0.32%			
FM15	4.003	3.988	0.016	0.39%	80.58	80.21	0.46%			
FM21	4.041	3.964	0.077	1.91%	71.52	69.87	2.31%	-132.3	-132.3	0.02
FM22	3.824	4.045	-0.221	-5.79%	202.69	209.73	-3.47%			
FM23	3.928	3.826	0.101	2.58%	181.27	178.36	1.61%			
FM26	3.815	3.729	0.085	2.24%	184.35	182.28	1.12%			
FM27	3.988	4.024	-0.036	-0.90%	72.27	73.11	-1.16%			
FM28	4.007	3.933	0.074	1.85%	35.41	34.44	2.76%			

Material: **FM steel-2**
Specimen type: **0.5TC(T)**

Specimen	Initial crack size, a_0 (mm)				Fracture toughness, K_{JC} (MPa√m)			Reference temperature, T_0 (°C)		
id	9ptA	AA	Δ		9ptA	AA	Δ	9ptA	AA	Δ
F55	12.009	12.008	0.001	0.01%	102.15	102.14	0.01%			
F56	11.979	12.034	-0.055	-0.46%	153.87	154.58	-0.46%			
F57	11.560	11.649	-0.089	-0.77%	191.93	193.13	-0.63%	-155.2	-155.0	-0.17
F58	12.542	12.361	0.181	1.44%	176.43	173.99	1.38%			
F59	11.706	11.614	0.092	0.79%	190.78	189.57	0.63%			
F5A	11.790	11.778	0.012	0.10%	44.34	44.28	0.14%			

Material: **FM steel-2**
Specimen type: **mini-bend bars**

Specimen	Initial crack size, a_0 (mm)				Fracture toughness, K_{Jc} (MPa√m)			Reference temperature, T_0 (°C)		
id	9ptA	AA	Δ		9ptA	AA	Δ	9ptA	AA	Δ
FB12	1.694	1.637	0.057	3.36%	56.53	54.34	3.86%			
FB13	1.644	1.646	-0.003	-0.15%	23.07	23.14	-0.30%			
FB14	1.625	1.607	0.018	1.10%	92.57	91.41	1.26%			
FB15	1.620	1.626	-0.006	-0.35%	142.19	142.47	-0.20%			
FB16	1.632	1.631	0.001	0.07%	55.16	55.12	0.08%			
FB21	1.619	1.619	0.000	0.00%	85.86	85.86	0.00%			
FB22	1.676	1.634	0.042	2.50%	97.20	95.07	2.19%			
FB23	1.615	1.600	0.015	0.93%	103.74	102.98	0.74%	-106.9	-106.4	-0.48
FB24	1.616	1.601	0.016	0.96%	152.12	151.44	0.45%			
FB25	1.606	1.589	0.017	1.05%	47.19	46.52	1.43%			
FB31	1.648	1.633	0.015	0.88%	76.22	75.62	0.79%			
FB32	1.613	1.609	0.003	0.21%	60.17	60.03	0.23%			
FB33	1.628	1.633	-0.005	-0.29%	79.28	79.47	-0.24%			
FB34	1.633	1.624	0.009	0.58%	59.81	59.44	0.61%			
FB35	1.601	1.573	0.028	1.74%	80.52	79.45	1.33%			
FB36	1.613	1.626	-0.013	-0.82%	96.73	97.25	-0.54%			

Material: **Biblis C base material**
Specimen type: **PCCv**

Specimen	Initial crack size, a_0 (mm)				Fracture toughness, K_{Jc} (MPa√m)			Reference temperature, T_0 (°C)		
id	9ptA	AA	Δ		9ptA	AA	Δ	9ptA	AA	Δ
B02-CV5	5.406	5.264	0.142	2.63%	64.61	62.53	3.22%			
B02-CV2	5.264	5.282	-0.018	-0.34%	61.51	61.80	-0.47%			
A08-CV5	5.121	5.144	-0.024	-0.46%	81.24	81.61	-0.45%			
B02-CV4	5.272	5.272	0.000	0.00%	74.38	74.38	0.00%			
A08-CV3	5.307	5.289	0.018	0.34%	68.59	68.31	0.41%	-14.9	-14.9	0.003
A08-CV1	5.192	5.215	-0.023	-0.45%	109.46	109.82	-0.33%			
A08-CV4	5.146	5.094	0.052	1.01%	102.95	102.09	0.83%			
A08-CV2	5.195	5.199	-0.004	-0.08%	94.04	94.10	-0.06%			
B02-CV1	5.242	5.231	0.012	0.22%	112.06	111.89	0.16%			
B02-CV3	5.157	5.177	-0.020	-0.39%	123.49	123.79	-0.24%			

Material: **Biblis C weld material**
Specimen type: **PCCv**

Specimen	Initial crack size, a_0 (mm)				Fracture toughness, K_{Jc} (MPa√m)			Reference temperature, T_0 (°C)		
id	9ptA	AA	Δ		9ptA	AA	Δ	9ptA	AA	Δ
D7-CV5	5.216	5.220	-0.003	-0.07%	103.05	103.12	-0.07%			
D3-CV4	5.098	5.092	0.007	0.13%	108.57	108.45	0.11%			
D3-CV1	5.273	5.273	0.000	0.00%	170.48	170.48	0.00%	-55.2	-55.2	0.007
D7-CV4	5.241	5.205	0.035	0.67%	248.91	248.08	0.33%			
D7-CV2	5.202	5.207	-0.005	-0.10%	353.18	353.33	-0.04%			

Material: **Biblis C weld material**
Specimen type: **SE(B) 20/40**

Specimen	Initial crack size, a_0 (mm)				Fracture toughness, K_{Jc} (MPa√m)			Reference temperature, T_0 (°C)		
id	9ptA	AA	Δ		9ptA	AA	Δ	9ptA	AA	Δ
SV2D3	21.083	20.882	0.201	0.95%	96.04	94.42	1.69%			
SV2C6	21.199	21.043	0.157	0.74%	91.16	90.24	1.01%			
SV2C2	20.983	20.905	0.078	0.37%	123.93	123.28	0.53%			
SV2B9	20.815	20.935	-0.120	-0.58%	254.74	255.81	-0.42%			
SV2D7	21.145	20.877	0.268	1.27%	130.00	127.67	1.79%	-89.7	-89.6	-0.083
SV2C10	20.910	21.162	-0.252	-1.21%	103.32	105.43	-2.05%			
SV2A4	21.261	21.089	0.172	0.81%	198.74	197.23	0.76%			
SV2B5	20.815	20.884	-0.069	-0.33%	202.37	202.96	-0.29%			
SV2B01	21.136	20.923	0.213	1.01%	245.13	243.30	0.75%			
SV2A08	20.733	20.655	0.079	0.38%	301.00	300.32	0.23%			

Appendix B. Detailed results for fully ductile tests (49 tests)

Material: **FZDR Round-Robin (2012)**
Specimen type: **1TC(T)**

Specimen	Initial crack size, a_0 (mm)				Final crack size, a_p (mm)				Crack extension, Δa_p (mm)				Single-specimen technique (Elastic Compliance)							
													Fracture toughness, J_Q (kJ/m^2)			Δa_{pred} - Δa_p		$\lvert a_{0q} - a_0 \rvert$	
id	9ptA	AA	Δ		9ptA	AA	Δ		9ptA	AA	Δ		9ptA	AA	Δ	9ptA	AA	9ptA	AA
BBL-CGW_23	25.071	24.940	0.131	0.52%	28.936	28.867	0.069	0.24%	3.865	3.927	-0.062	-1.60%	847.28	847.28	0.00%	YES	YES	YES	YES
BBL-CGW_24	25.189	25.086	0.103	0.41%	29.141	28.398	0.742	2.55%	3.951	3.312	0.639	16.17%	630.97	630.97	0.00%	YES	YES	NO	YES
BBL-CGW_24	25.386	25.119	0.267	1.05%	29.071	28.630	0.440	1.52%	3.685	3.512	0.173	4.71%	887.32	887.32	0.00%	YES	YES	NO	NO

Material: **AM Ti64**
Specimen type: **PCCv**

Specimen	Initial crack size, a_0 (mm)				Final crack size, a_p (mm)				Crack extension, Δa_p (mm)				Single-specimen technique (Elastic Compliance)							Single-Specimen technique (NDR)		
													Fracture toughness, J_Q (kJ/m^2)			Δa_{pred} - Δa_p		$\lvert a_{0q} - a_0 \rvert$		Fracture toughness, J_Q (kJ/m^2)		
id	9ptA	AA	Δ		9ptA	AA	Δ		9ptA	AA	Δ		9ptA	AA	Δ	9ptA	AA	9ptA	AA	9ptA	AA	Δ
900HIP_4_N_a	4.987	4.967	0.020	0.41%	8.306	8.282	0.024	0.29%	3.319	3.315	0.004	0.11%	178.06	178.04	0.01%	NO	NO	YES	YES	122.99	124.02	-0.8%
900HIP_4_N_b	4.805	4.836	-0.031	-0.64%	5.958	6.046	-0.088	-1.48%	1.153	1.210	-0.058	-5.02%	179.14	179.15	0.00%	NO	NO	YES	YES	104.45	103.51	0.9%
900HIP_4_N_c	5.089	5.131	-0.043	-0.84%	9.086	9.083	0.004	0.04%	3.998	3.951	0.046	1.16%	140.11	140.11	-0.01%	NO	NO	YES	YES			
900HIP_4_S_a	5.072	5.080	-0.008	-0.16%	7.119	7.133	-0.015	-0.21%	2.047	2.054	-0.007	-0.33%	190.70	190.70	0.00%	NO	NO	YES	YES	120.54	120.41	0.1%
900HIP_4_S_b	5.030	5.080	-0.050	-0.99%	7.509	7.534	-0.025	-0.33%	2.479	2.454	0.025	1.00%	156.63	156.63	0.00%	YES	YES	YES	YES	164.74	182.69	-10.9%
900HIP_4_S_c	5.210	5.199	0.011	0.21%	7.130	7.113	0.017	0.23%	1.920	1.915	0.006	0.29%	186.04	186.04	0.00%	YES	YES	YES	YES	197.78	197.81	0.0%

Material: **X100 Weld Metal**
Specimen type: **SE(B) 12.5/25**

Specimen	Initial crack size, a_0 (mm)				Final crack size, a_p (mm)				Crack extension, Δa_p (mm)				Single-specimen technique (Elastic Compliance)						
													Fracture toughness, J_Q (kJ/m^2)			Δa_{pred} - Δa_p		$\lvert a_{0q} - a_0 \rvert$	
id	9ptA	AA	Δ		9ptA	AA	Δ		9ptA	AA	Δ		9ptA	AA	Δ	9ptA	AA	9ptA	AA
DW1	12.904	12.852	0.052	0.40%	14.819	14.583	0.236	1.59%	1.915	1.731	0.184	9.59%	279.32	279.32	0.00%	NO	NO	YES	YES
DW3	12.726	12.644	0.082	0.65%	15.304	15.195	0.109	0.71%	2.578	2.551	0.027	1.05%	242.05	242.05	0.00%	NO	NO	YES	YES
DW6	12.878	12.692	0.186	1.44%	13.883	13.557	0.326	2.35%	1.005	0.865	0.140	13.96%	293.13	293.13	0.00%	NO	YES	YES	YES
FW1	12.826	12.685	0.141	1.10%	15.072	14.805	0.267	1.77%	2.246	2.121	0.126	5.60%	279.69	279.68	0.00%	NO	NO	YES	YES
FW3	12.842	12.727	0.115	0.90%	15.501	14.794	0.706	4.56%	2.659	2.068	0.591	22.23%	220.48	220.48	0.00%	NO	YES	YES	YES
FW6	12.833	12.739	0.094	0.73%	15.058	14.805	0.253	1.68%	2.225	2.066	0.159	7.14%	274.15	274.15	0.00%	NO	NO	YES	YES

Material: **SH-38 multi-specimen & PD**
Specimen type: **PCCv, 20 % side-grooved**

Specimen	Initial crack size, a_0 (mm)				Final crack size, a_p (mm)				Crack extension, Δa_p (mm)				Multi-Specimen technique						Single-Specimen technique (DCEPD)			Normalization Data Reduction		
													Multi-specimen J-int (kJ/m^2)			Fracture toughness, J_Q (kJ/m^2)			Fracture toughness, J_Q (kJ/m^2)			Fracture toughness, J_Q (kJ/m^2)		
id	9ptA	AA	Δ		9ptA	AA	Δ		9ptA	AA	Δ		9ptA	AA	Δ	9ptA	AA	Δ	9ptA	AA	Δ	9ptA	AA	Δ
PCVN-1	5.335	5.365	-0.030	-0.55%	5.801	5.904	-0.103	-1.77%	0.466	0.540	-0.073	-15.74%	590.71	591.47	-0.13%									
PCVN-2	5.484	5.490	-0.006	-0.11%	6.324	6.423	-0.099	-1.56%	0.841	0.933	-0.093	-11.02%	804.58	800.68	0.48%				601.14	515.04	14.3%	354.95	335.83	5.4%
PCVN-3	5.125	5.159	-0.034	-0.66%	5.894	5.982	-0.088	-1.49%	0.769	0.823	-0.054	-7.00%	818.28	821.41	-0.38%	640.65	569.39	11.1%	687.31	622.09	9.5%	610.80	616.25	-0.9%
PCVN-4	4.979	5.017	-0.038	-0.77%	5.585	5.717	-0.132	-2.35%	0.606	0.700	-0.093	-15.40%	739.76	741.59	-0.25%				692.07	565.51	18.3%			
PCVN-5	5.396	5.382	0.014	0.26%	5.913	5.970	-0.058	-0.98%	0.516	0.588	-0.072	-13.90%	675.67	670.29	0.80%									

Material: **SH-38 multi-specimen**
Specimen type: **PCCv, plain-sided**

Specimen	Initial crack size, a_0 (mm)				Final crack size, a_p (mm)				Crack extension, Δa_p (mm)				Multi-Specimen technique					
													Multi-specimen J-int (kJ/m^2)			Fracture toughness, J_Q (kJ/m^2)		
id	9ptA	AA	Δ		9ptA	AA	Δ		9ptA	AA	Δ		9ptA	AA	Δ	9ptA	AA	Δ
SH-29	5.227	5.299	-0.072	-1.37%	6.474	6.537	-0.063	-0.97%	1.247	1.238	0.009	0.69%	1472.17	1493.81	-1.47%			
SH-42	5.195	5.215	-0.019	-0.37%	5.770	5.797	-0.027	-0.47%	0.575	0.583	-0.008	-1.34%	937.84	941.06	-0.34%	978.00	1023.25	-4.6%
SH-135	5.256	5.368	-0.112	-2.13%	6.329	6.331	-0.002	-0.03%	1.073	0.963	0.110	10.27%	1273.77	1311.57	-2.97%			
SH-219	4.835	4.822	0.014	0.28%	6.346	6.430	-0.084	-1.32%	1.511	1.609	-0.098	-6.46%	978.00	1023.25	-4.63%			

Material: **X65 multi-specimen & PD**
Specimen type: **PCCv, 20 % side-grooved**

Specimen	Initial crack size, a_0 (mm)				Final crack size, a_p (mm)				Crack extension, Δa_p (mm)				Multi-Specimen technique						Single-Specimen technique (DCEPD)			Normalization Data Reduction		
													Multi-specimen J-int (kJ/m^2)			Fracture toughness, J_Q (kJ/m^2)			Fracture toughness, J_Q (kJ/m^2)			Fracture toughness, J_Q (kJ/m^2)		
id	9ptA	AA	Δ		9ptA	AA	Δ		9ptA	AA	Δ		9ptA	AA	Δ	9ptA	AA	Δ	9ptA	AA	Δ	9ptA	AA	Δ
V1	4.581	4.635	-0.054	-1.19%	6.222	6.195	0.027	0.43%	1.641	1.559	0.081	4.95%	1434.07	1454.01	-1.39%							783.25	811.27	-3.6%
V2	4.816	4.923	-0.107	-2.22%	7.442	7.301	0.141	1.89%	2.626	2.378	0.248	9.43%	1921.79	1984.22	-3.25%									
V3	4.900	4.944	-0.045	-0.91%	6.128	6.101	0.027	0.44%	1.228	1.157	0.072	5.83%	1137.09	1151.42	-1.26%									
V4	4.854	4.960	-0.106	-2.19%	6.926	6.848	0.078	1.12%	2.072	1.888	0.184	8.88%	1697.80	1748.26	-2.97%							1681.86	1763.50	-4.9%
V5	4.864	4.898	-0.034	-0.69%	8.437	8.185	0.252	2.98%	3.573	3.287	0.285	7.99%	2250.27	2297.29	-2.09%							1182.77	1472.49	-24.5%
V6	4.810	4.864	-0.054	-1.13%	7.280	7.121	0.159	2.18%	2.470	2.257	0.213	8.63%	1791.80	1830.27	-2.15%							1649.92	1272.34	22.9%
V7	4.589	4.651	-0.062	-1.35%	6.560	6.402	0.158	2.41%	1.971	1.751	0.220	11.16%	1560.94	1596.63	-2.29%							1346.86	1023.61	24.0%
V8	4.686	4.731	-0.045	-0.97%	7.449	7.176	0.272	3.65%	2.763	2.445	0.317	11.49%	1967.63	2016.82	-2.50%	1034.66	1107.44	-7.0%				1718.42	1848.50	-7.6%
V9	4.824	4.828	-0.004	-0.08%	6.193	6.140	0.053	0.85%	1.369	1.312	0.056	4.11%	1317.47	1322.72	-0.40%							1239.76	1313.22	-5.9%
V10	4.612	4.645	-0.033	-0.72%	6.124	6.062	0.062	1.01%	1.512	1.417	0.095	6.26%	1403.09	1418.74	-1.12%									
V12	4.856	4.848	0.008	0.17%	5.300	5.315	-0.015	-0.27%	0.444	0.467	-0.023	-5.19%	544.61	542.93	0.31%				390.35	384.42	1.5%			
V14	5.364	5.355	0.009	0.16%	5.948	5.948	0.001	0.01%	0.584	0.593	-0.008	-1.39%	695.07	693.39	0.24%									
V13	5.434	5.456	-0.022	-0.40%	5.795	5.935	-0.140	-2.42%	0.361	0.480	-0.119	-32.97%	608.86	606.76	0.35%									
V15	5.059	5.046	0.013	0.26%	6.009	5.965	0.045	0.75%	0.950	0.918	0.032	3.32%	841.18	840.65	0.06%									
V20	5.216	5.160	0.055	1.06%	5.944	5.947	-0.003	-0.05%	0.728	0.786	-0.058	-8.01%	782.54	770.84	1.50%									

Material: **SH-38 multi-specimen**
Specimen type: **PKLST, plain-sided**

Specimen	Initial crack size, a_0 (mm)				Final crack size, a_p (mm)				Crack extension, Δa_p (mm)				Multi-Specimen technique					
													Multi-specimen J-int (kJ/m^2)			Fracture toughness, J_Q (kJ/m^2)		
id	9ptA	AA	Δ		9ptA	AA	Δ		9ptA	AA	Δ		9ptA	AA	Δ	9ptA	AA	Δ
SH38-K1	1.874	1.920	-0.046	-2.46%	3.396	3.301	0.095	2.80%	1.522	1.381	0.141	9.29%	357.61	364.94	-2.05%			
SH38-K2	1.973	2.009	-0.036	-1.82%	2.115	2.134	-0.018	-0.87%	0.142	0.125	0.018	12.33%	723.52	736.04	-1.73%			
SH38-K3	2.060	2.081	-0.021	-1.04%	2.608	2.584	0.024	0.90%	0.548	0.503	0.045	8.19%	802.73	811.18	-1.05%	658.37	719.85	-9.3%
SH38-K4	2.031	2.003	0.029	1.41%	2.964	2.774	0.190	6.40%	0.932	0.771	0.161	17.29%	966.25	994.26	-2.90%			
SH38-K5	1.947	1.984	-0.037	-1.91%	3.253	3.191	0.062	1.90%	1.306	1.208	0.099	7.57%	1224.64	1269.80	-3.69%			

Material: **X65 multi-specimen**
Specimen type: **PKLST, plain-sided**

Specimen	Initial crack size, a_0 (mm)				Final crack size, a_p (mm)				Crack extension, Δa_p (mm)				Multi-Specimen technique					
													Multi-specimen J-int (kJ/m^2)			Fracture toughness, J_Q (kJ/m^2)		
id	9ptA	AA	Δ		9ptA	AA	Δ		9ptA	AA	Δ		9ptA	AA	Δ	9ptA	AA	Δ
X65-K1	1.859	1.824	0.035	1.86%	2.044	1.991	0.053	2.60%	0.186	0.167	0.018	9.94%	349.68	345.04	1.33%			
X65-K2	1.843	1.820	0.023	1.23%	2.322	2.273	0.049	2.10%	0.479	0.453	0.026	5.45%	666.71	662.53	0.63%			
X65-K3	1.809	1.802	0.007	0.38%	2.382	2.335	0.047	1.96%	0.573	0.533	0.040	6.93%	648.01	649.58	-0.24%	671.00	698.99	-4.2%
X65-K4	1.904	1.872	0.032	1.66%	2.752	2.713	0.040	1.44%	0.849	0.840	0.008	0.96%	1029.03	1016.55	1.21%			
X65-K5	1.846	1.850	-0.004	-0.19%	3.059	2.972	0.087	2.83%	1.213	1.122	0.090	7.45%	1246.32	1262.95	-1.33%			

References

[1] Annual Book of ASTM Standards, Volume 03.01 Metals – Mechanical Testing; Elevated and Low Temperature Tests; Metallography, ASTM International, West Conshohocken, PA, July 2021.

[2] ASTM E647-15$^{\varepsilon 1}$, Standard Test Method for Measurement of Fatigue Crack Growth Rates, Annual Book of ASTM Standards, Vol. 03.01, ASTM International, West Conshohocken, PA, July 2021.

[3] ASTM E1457-19$^{\varepsilon 1}$, Standard Test Method for Measurement of Creep Crack Growth Times in Metals, Annual Book of ASTM Standards, Vol. 03.01, ASTM International, West Conshohocken, PA, July 2021.

[4] ASTM E399-20^{a}, Standard Test Method for Linear-Elastic Plane-Strain Fracture Toughness of Metallic Materials, Annual Book of ASTM Standards, Vol. 03.01, ASTM International, West Conshohocken, PA, July 2021.

[5] ASTM E561-20, Standard Test Method for KR Curve Determination, Annual Book of ASTM Standards, Vol. 03.01, ASTM International, West Conshohocken, PA, July 2021.

[6] ASTM E1221-12a(2018), Standard Test Method for Determining Plane-Strain Crack-Arrest Fracture Toughness, KIa, of Ferritic Steels, Annual Book of ASTM Standards, Vol. 03.01, ASTM International, West Conshohocken, PA, July 2021.

[7] ASTM E2472-12(2018)$^{\varepsilon 1}$, Standard Test Method for Determination of Resistance to Stable Crack Extension under Low-Constraint Conditions, Annual Book of ASTM Standards, Vol. 03.01, ASTM International, West Conshohocken, PA, July 2021.

[8] ASTM E1681-03(2020), Standard Test Method for Determining Threshold Stress Intensity Factor for Environment-Assisted Cracking of Metallic Materials, Annual Book of ASTM Standards, Vol. 03.01, ASTM International, West Conshohocken, PA, July 2021.

[9] ISO 12737:2005(E), Metallic Materials — Determination of plane-strain fracture toughness, second ed., International Standards Organization, Geneva (Switzerland), 2005.

[10] ASTM E2760-19$^{\varepsilon 1}$, Standard Test Method for Creep-Fatigue Crack Growth Testing, Annual Book of ASTM Standards, Vol. 03.01, ASTM International, West Conshohocken, PA, July 2021.

[11] ASTM E1921-21, Standard Test Method for Determination of Reference Temperature, T0, for Ferritic Steels in the Transition Range, Annual Book of ASTM Standards, Vol. 03.01, ASTM International, West Conshohocken, PA, July 2021.

[12] ASTM E1820-20b, Standard Test Method for Measurement of Fracture Toughness, Annual Book of ASTM Standards, Vol. 03.01, ASTM International, West Conshohocken, PA, July 2021.

[13] Kim Wallin, The Scatter in K_{Ic} Results, Eng. Fract. Mech. 19 (6) (1984) 1085–1093.

[14] Caroline A Schneider, Wayne S Rasband, Kevin W Eliceiri, NIH Image to ImageJ: 25 years of image analysis, Nat. Meth. 9 (7) (2012) 671–675.
[15] Tony J. Collins, ImageJ for microscopy, BioTechniques 43 (1S) (2007) S25–S30.
[16] K.C. Lieb, R. Horstman, K.A. Peters, R.L. Meltzer, M.B. Vieth, G.A. Clarke, J. D. Landes, J.A. Begley, Results of an ASTM Cooperative Test Program on the J_{Ic} Determination of HY-130 Steel, J. Test. Eval. 8 (5) (1980) 221, https://doi.org/10.1520/JTE10614J.